DALTON
FULL PAPER

Reactions of nickelocene with an Ru_5 cluster: crystal structures of two nickel–ruthenium clusters containing C_2 ligands

Chris J. Adams,[a] Michael I. Bruce,[a] Jean-François Halet,[b] Samia Kahlal,[b] Brian W. Skelton[c] and Allan H. White[c]

[a] *Department of Chemistry, University of Adelaide, Adelaide, South Australia 5005, Australia. E-mail: michael.bruce@adelaide.edu.au*
[b] *Laboratoire de Chimie du Solide et Inorganique Moléculaire, UMR CNRS 6511, Université de Rennes 1, Institut de Chimie de rennes, 35042 Rennes Cedex, France. E-mail: halet@univ-rennes1.fr*
[c] *Department of Chemistry, University of Western Australia, Nedlands, Western Australia 6009, Australia*

Received 29th June 2000, Accepted 7th December 2000
First published as an Advance Article on the web 31st January 2001

Reactions of nickelocene with $Ru_5(\mu_5\text{-}C_2)(\mu\text{-}SMe)_2(\mu\text{-}PPh_2)_2(CO)_{11}$ have given $NiRu_5(\mu_6\text{-}C_2)(\mu\text{-}SMe)_2(\mu\text{-}PPh_2)_2(CO)_9Cp_2$ and $Ni_2Ru_4(\mu_6\text{-}C_2)(\mu\text{-}SMe)_2(\mu\text{-}PPh_2)_2(CO)_8Cp_2$ whose molecular structures have been determined. The $NiRu_5$ cluster is related to other heterometallic clusters containing $FeRu_5$, Ru_6 or Co_2Ru_5 cores which contain two edge-fused squares supporting the C_2 ligand, one carbon occupying the centre of each square face while retaining the C–C bond. However, there is no formal M–M interaction along the shared edge. Substitution of CO groups by Cp on one Ru atom has occurred. The structure of the Ni_2Ru_4 cluster is similar, with the six-membered ring having the boat conformation. The C_2 ligand takes up two disordered (1 : 1) positions, either parallel or perpendicular to the non-bonding Ni · · · Ni vector. Extended Hückel and density functional calculations have been carried out on $Ni_2Ru_4(\mu_6\text{-}C_2)(\mu\text{-}SMe)_2(\mu\text{-}PPh_2)_2(CO)_8Cp_2$ to rationalise these two observed coordination modes of the C_2 unit to the metal framework. Results suggest that the two arrangements are isoenergetic and that the M–C bonding follows the Dewar–Chatt–Duncanson model as previously found for related C_2-containing polynuclear organometallic clusters.

Introduction

In previous papers[1,2] we have described some of the homo- and hetero-metallic clusters which can be obtained by adding appropriate metal substrates to the open dicarbon cluster $Ru_5(\mu_5\text{-}C_2)(\mu\text{-}SMe)_2(\mu\text{-}PPh_2)_2(CO)_{11}$ **1**. These include the complexes $MRu_5(\mu_6\text{-}C_2)(\mu\text{-}SMe)_2(\mu\text{-}PPh_2)_2(CO)_{14}$ **2** and $M_2Ru_5(\mu_6\text{-}C_2)(\mu_3\text{-}SMe)_2(\mu\text{-}PPh_2)_2(\mu\text{-}CO)(CO)_{15}$ **3** (M = Fe or Ru) obtained from iron or ruthenium carbonyls and $Co_2Ru_6(\mu_7\text{-}C_2)(\mu_3\text{-}SMe)_2(\mu\text{-}PPh_2)_2(\mu\text{-}CO)_4(CO)_{13}$ **4** and $Co_4Ru_5(\mu_8\text{-}C_2)(\mu_3\text{-}SMe)_2(\mu\text{-}PPh_2)_2(\mu\text{-}CO)_7(CO)_{11}$ **5**, which were formed with $Co_2(CO)_8$. The common feature of these structures was the presence of six metals as a pair of edge-fused squares (permetalla[2.2.0]hexane framework) which supported the C_2 ligand by virtue of each carbon being attached in the centre of a square face, retaining the C–C bond [which varied in length between 1.355(9) and 1.41(4) Å].

Several other clusters containing C_2 ligands with extensive interactions with the cluster cores have been described. An incomplete list containing those relevant to the present paper includes unusual C_2-containing clusters obtained from reactions of $\{Fe(CO)_2Cp^*\}_2(\mu\text{-}C_2)$ with $Ru_3(CO)_{12}$, including $Ru_5\{\mu_4\text{-}C_2[Fe(CO)_2Cp^*]\}_2(CO)_{13}$ **6**, $FeRu_6(\mu_5\text{-}C_2)(\mu_4\text{-}C_2H)(CO)_{16}Cp$ **7** and $Fe_2Ru_6(\mu_6\text{-}C_2)_2(\mu\text{-}CO)_3(CO)_{14}Cp^*_2$ **8**, described by Akita, Moro-oka and co-workers.[3,4] The cluster $Co_6(\mu_6\text{-}C_2)(\mu_4\text{-}S)(\mu\text{-}CO)_6(CO)_8$ **9** is a minor product from the reaction of $Co_2(CO)_8$ with CS_2[5] and the cluster anion $[Co_3Fe_3(\mu_6\text{-}C_2)(CO)_{18}]^-$ **10** was obtained from $[Fe_3(\mu_3\text{-}C_2OAc)(CO)_9]^-$ and $[Fe(CO)_4]^{2-}$, followed by $Co_2(CO)_8$.[6] Two Co_3 clusters linked by a C_2 moiety are found in $\{Co_3(CO)_9\}_2(\mu_3\text{:}\mu_3\text{-}C_2)$ **11**.[7] This paper describes two complexes obtained from the reactions of **1** with nickelocene, having an M_6C_2 framework related to those found in **2**, **8** and **9**.

Results

If a mixture of nickelocene and compound **1** is heated in toluene at 120 °C for 1 h, separation of the reaction products by preparative thin-layer chromatography affords dark brown $NiRu_5(\mu_6\text{-}C_2)(\mu\text{-}SMe)_2(\mu\text{-}PPh_2)_2(CO)_9Cp_2$ **12** and green $Ni_2Ru_4(\mu_6\text{-}C_2)(\mu\text{-}SMe)_2(\mu\text{-}PPh_2)_2(CO)_8Cp_2$ **13** in (Scheme 1) 7 and 9% yields, respectively, both of which have been characterised by single-crystal X-ray structural studies. The yield of the Ni_2Ru_4 complex increases to 15% after 18 h. The low yields have precluded our obtaining ^{13}C NMR spectra. Both complexes have all-terminal ν(CO) IR spectra between 2030 and 1950 cm^{-1}. In the ^1H NMR spectrum of **13** two equal intensity singlet resonances for the Cp protons were found at δ 5.89 and 6.01, while the SMe groups gave rise to two singlets at δ 1.31 and 1.65. Molecular ions were found in the mass spectra of both complexes.

Molecular structures

(a) $NiRu_5(\mu_6\text{-}C_2)(\mu\text{-}SMe)_2(\mu\text{-}PPh_2)_2(CO)_9Cp_2$ 12. A plot of a molecule of compound **12** is shown in Fig. 1 and selected structural parameters are collected in Table 1. As can be seen, the permetallabicyclo[2.2.0]hexane skeleton found in **2**[1] has opened to a permetallacyclohexane by virtue of the long, essentially non-bonding Ni(5) · · · Ru(2) hinge distance of 3.505(1) Å. The Ru–Ru separations form two groups, those spanned by the PPh_2 groups, which are longer [2.9416, 2.9455(7) Å] than the other, non-bridged edges [2.8379, 2.8481(7) Å]. Bonds involving Ni(5) are the two edges [2.6443, 2.6590(9) Å]. The two outer edges are each bridged by a PPh_2 group [Ru–P 2.295–2.313(2) Å] and the two SMe groups span the non-bonded Ru(1) · · · Ru(3) and Ru(4) · · · Ru(6) vectors [Ru–S 2.459–2.475(1) Å].

 DOI: 10.1039/b005210h

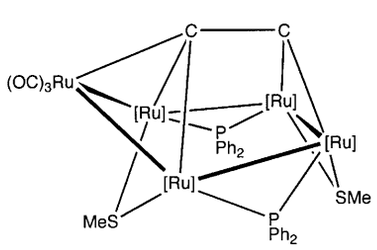

(**1**) [Ru] = $Ru(CO)_2$

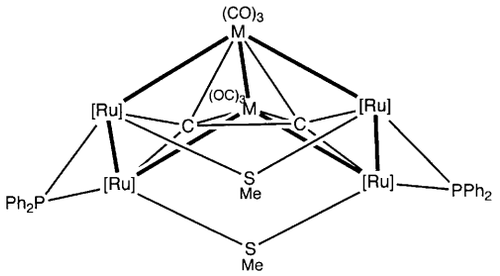

(**2**) [Ru] = $Ru(CO)_2$; M = Fe, Ru

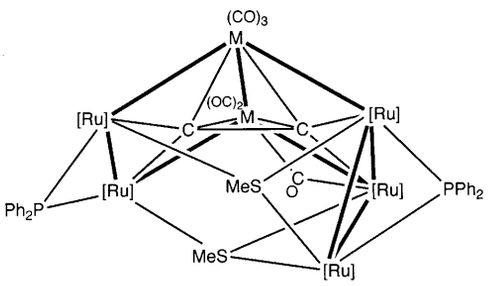

(**3**) [Ru] = $Ru(CO)_2$; M = Fe, Ru

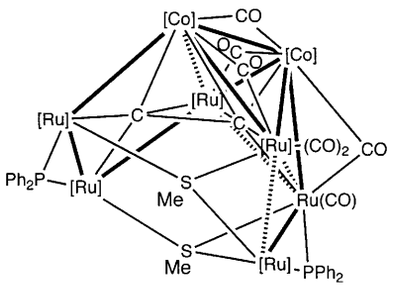

(**4**) [Co] = Co(CO), [Ru] = $Ru(CO)_2$

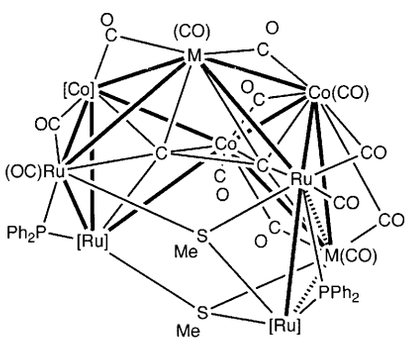

(**5**) [Co] = Co(CO), [Ru] = $Ru(CO)_2$, M = Co, Ru

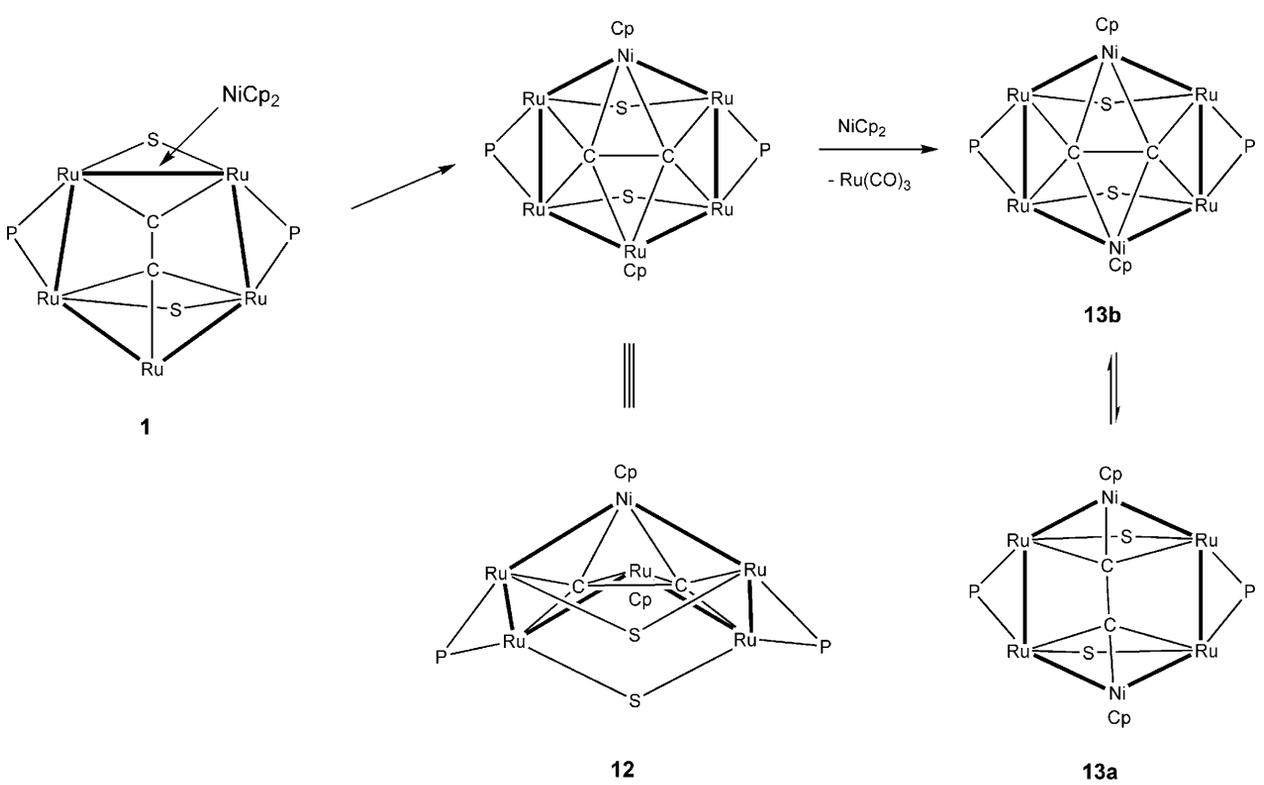

Scheme 1

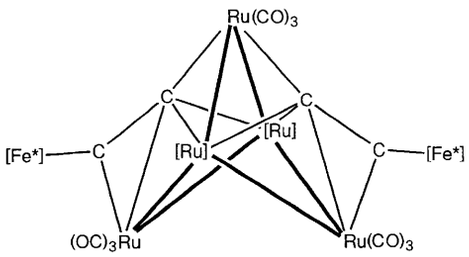

6 [Fe*] = $Fe(CO)_2Cp^*$, [Ru] = $Ru(CO)_2$

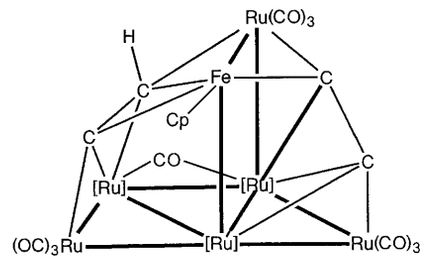

7 [Ru] = $Ru(CO)_2$

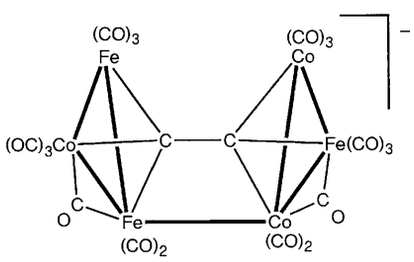

10

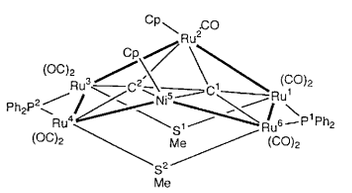

12

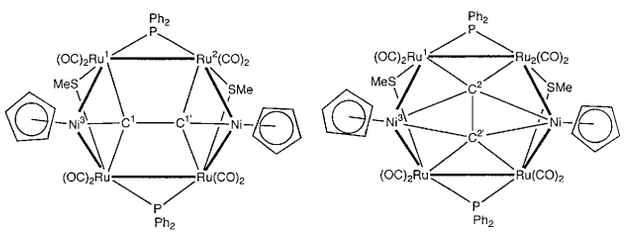

13

The two $NiRu_3$ planes (χ^2 4950, 9789) are inclined at an angle of 90.37(3)° and each is slightly irregular, with internal angles at Ni of 86.91 and 86.95(2)° and at Ru of 95.36–96.16(2)°, as expected from the long Ni···Ru separation.

The two hinge atoms each carry a Cp group [average M–C(Cp) 2.147 (Ni), 2.226 Å (Ru)]. The C_2 ligand spans the approximate centres of the two faces [Ni–C 2.017–2.030(6) Å; Ru–C 2.163–2.199(6) Å] with a C(1)–C(2) distance of 1.328(7) Å. The C–C bond is inclined at angles of 44.69 and 44.95(2)° to the mean planes of the two $NiRu_3$ faces. Coordination of the ruthenium atoms is completed by two terminal CO groups to each one except for Ru(2) which has one.

(b) $Ni_2Ru_4(\mu_6\text{-}C_2)(\mu\text{-}SMe)_2(\mu\text{-}PPh_2)_2(CO)_8Cp_2$ 13. Here, one-half of the molecule is crystallographically independent, a

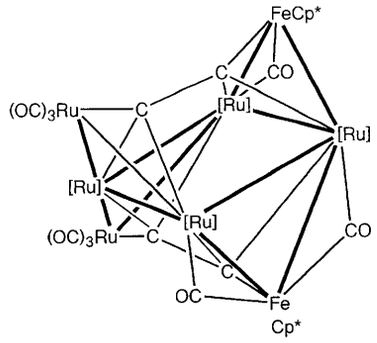

8 [Ru] = $Ru(CO)_2$

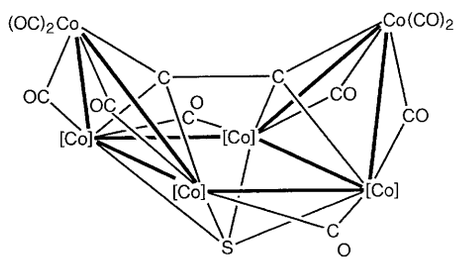

9 [Co] = Co(CO)

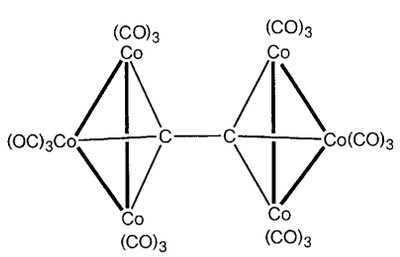

11

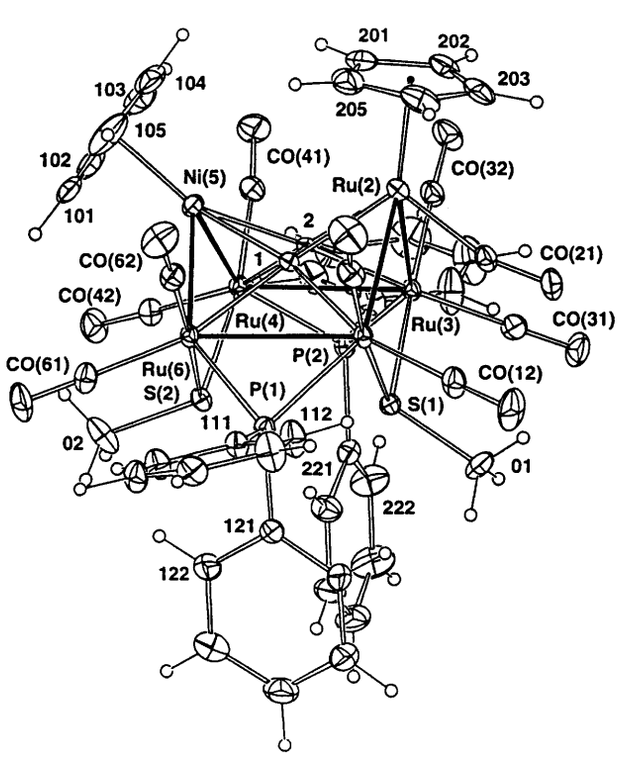

Fig. 1 Projection of $NiRu_5(\mu_6\text{-}C_2)(\mu\text{-}SMe)_2(\mu\text{-}PPh_2)_2(CO)_9Cp_2$ **12** oblique to the Ru_4 plane. 20% Thermal ellipsoids are shown for the non-hydrogen atoms.

crystallographic 2 axis lying through the centre of and normal to the Ru_4 plane (χ^2 385). The metal skeleton is similar to that of compound **12** and consists of a permetallacyclohexane in the

Table 1 Selected structural data (distances in Å, angles in °) for $NiRu_5(\mu_6\text{-}C_2)(\mu\text{-}SMe)_2(\mu\text{-}PPh_2)_2(CO)_9Cp_2$ **12**

Ru(1)–Ru(2)	2.8379(7)	Ru(1)–C(1)	2.199(6)
Ru(1)–Ru(6)	2.9455(7)	Ru(2)–C(1)	2.170(5)
Ru(2)–Ru(3)	2.8481(7)	Ru(6)–C(1)	2.163(5)
Ru(3)–Ru(4)	2.9416(7)	Ru(2)–C(2)	2.173(6)
Ru(2)···Ni(5)	3.505(1)	Ru(3)–C(2)	2.184(5)
Ru(4)–Ni(5)	2.6590(9)	Ru(4)–C(2)	2.166(6)
Ru(6)–Ni(5)	2.6443(9)	Ni(5)–C(1)	2.017(6)
Ru(1)–S(1)	2.459(2)	Ni(5)–C(2)	2.030(5)
Ru(3)–S(1)	2.475(1)	C(1)–C(2)	1.328(7)
Ru(4)–S(2)	2.469(1)		
Ru(6)–S(2)	2.461(2)		
Ru(1)–P(1)	2.303(2)	Ru(1)–S(1)–Ru(3)	101.94(5)
Ru(6)–P(1)	2.295(2)	Ru(4)–S(2)–Ru(6)	103.58(6)
Ru(3)–P(2)	2.312(2)		
Ru(4)–P(2)	2.313(2)	Dihedral angles	
Ru(2)–C(Cp)	2.207–2.246(9)	Ru(2,1,6)Ni(5)/Ru(2,3,4)Ni(5)	90.37(3)
av.	2.23	Ru(2,1,6)Ni(5)/C(1,2)	44.69(2)
Ni(5)–C(Cp)	2.09(1)–2.232(8)	Ru(2,3,4)Ni(5)/C(2,1)	44.95(2)
av.	2.15		
Other distances:	C(1) from Ru(2,1,6)Ni(5) mean plane	0.200(6)	
	C(2) from Ru(2,3,4)Ni(5) mean plane	0.190(6)	

Table 2 Selected structural data (distances in Å, angles in °) for $Ni_2Ru_4(\mu_6\text{-}C_2)(\mu\text{-}SMe)_2(\mu\text{-}PPh_2)_2(CO)_8Cp_2$ **13**. Pertinent DFT computed bond lengths are given in square brackets for comparison

	13a	**13b**	
Ru(1)–Ru(2)	2.944(2) [2.993]		2.944(2) [2.938]
Ru(1)···Ru(2*)	3.576(2) [3.454]		3.576(2) [3.827]
Ru(1)–Ni(3)	2.690(8) [2.635]		
Ru(1)–Ni(3′)			2.582(9) [2.689]
Ru(2)–Ni(3*)	2.678(9) [2.631]		2.678(9) [2.657]
Ru(2)–Ni(3′)			2.589(9) [2.657]
Ni(3)···Ni(3*)	4.835(8) [4.636]	Ni(3′)···Ni(3′*)	3.471(9) [3.370]
Ru(1)–S	2.430(4) [2.464]		2.430(4) [2.487]
Ru(2)–S*	2.426(4) [2.457]		2.426(4) [2.482]
Ru(1)–P	2.294(5) [2.327]		2.294(5) [2.310]
Ru(2)–P	2.299(4) [2.329]		2.299(4) [2.311]
Ru(1)–C(1)	2.32(3) [2.256]	Ru(1)–C(2)	2.14(3) [2.194]
Ru(2)–C(1*)	2.24(3) [2.237]	Ru(2)–C(2)	2.18(4) [2.191]
Ni(3)–C(1)	1.72(3) [1.782]	Ni(3′)–C(2)	1.97(4) [1.969]
Ni(3*)–C(1*)	1.72(3) [1.780]	Ni(3′)–C(2*)	2.05(4) [2.000]
C(1)–C(1*)	1.57(4) [1.316]	C(2)–C(2*)	1.16(4) [1.330]
Ni(3)–C(Cp)	1.81(5)–2.06(4) [2.108–2.115]	Ni(3′)–C(Cp)	2.08(6)–2.47(5) [2.112–2.181]
av.	1.98 [2.112]		2.30 [2.146]
Ru(1)–Ni(3)–Ru(2)	83.6(2)	Ru(1)–Ni(3′)–Ru(2*)	87.5(3)
Ni(3)–C(1)–C(1′)	162(2)		
Dihedral angles			
Ru(1,2,2′,1′)/Ni(3)Ru(1,2*)	61.8(3)	Ru(1,2,2′,1′)/Ni(3′)Ru(1,2)	81.9(3)

The asterisks denote atoms generated by the intracluster crystallographic 2 axis.

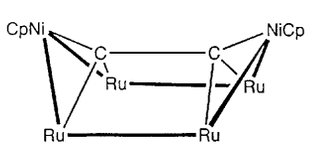

13a

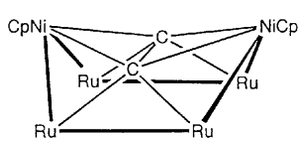

13b

boat conformation. Atoms Ru(1) and Ru(2) [Ru–Ru 2.944(2) Å] are bridged by the PPh_2 groups [Ru–P 2.294(5) Å], and the non-bonding Ru···Ru vectors [Ru···Ru 3.576(2) Å] are bridged by the two SMe groups [Ru–S 2.430(4), 2.426(4) Å]. The nickel atoms are disordered over two sites (Ni, Ni′), each with equal occupancy, such that Ru–Ni is 2.690(8) Å and Ru–Ni′ is 2.582(9) Å; the Ni···Ni′ separation is 0.687(8) Å. The Ni···Ni and Ni′···Ni′ hinge distances are 4.835(8) and 3.471(9) Å, respectively, which suggests that the bonding interaction between them is at best very weak. The interplanar angles $NiRu_2/Ru_4$ are 61.8(3) (Ni) and 81.9(3)° (Ni′). Each Ru atom carries two terminal CO groups and the two nickel atoms are each coordinated by a Cp group.

The C_2 ligand is also disordered over two sites, such that the two C–C axes are mutually orthogonal: in **13a** the C–C axis is parallel to the Ni···Ni′ vector, whereas in **13b** it is orthogonal to this vector. These structures are shown in Fig. 2: the relevant bond distances (Table 2) for **13a**, **13b** are: Ru(1)–C(1) 2.32, Ru(2)–C(1*) 2.24(3), Ni(3)–C(1) 1.72(3), C(1)–C(1*) 1.57(4) Å for **13a**; Ru(1,2)–C(2) 2.14, 2.18(4), Ni(3′)–C(2) 1.97(4), Ni(3′)–C(2*) 2.05(4), C(2)–C(2*) 1.16(4) Å for **13b**. Although the esds are high, the C(1)–C(1′) distance is longer than C(2)–C(2*), consistent with the latter being attached to Ni(3′) in the $\mu\text{-}\eta^2\text{:}\eta^2\text{-}C_2$ mode, while C(1)–C(1*) are attached to Ni(3) in the $\mu\text{-}\eta^1\text{:}\eta^1\text{-}C_2$ mode. These structural arrangements are illustrated; the alternatives result in short Ni(3′)–C(1) distances [1.13(3) Å] and overlong Ni(3,3′)–C(2) distances [2.56, 2.64(4) Å]. In both cases we

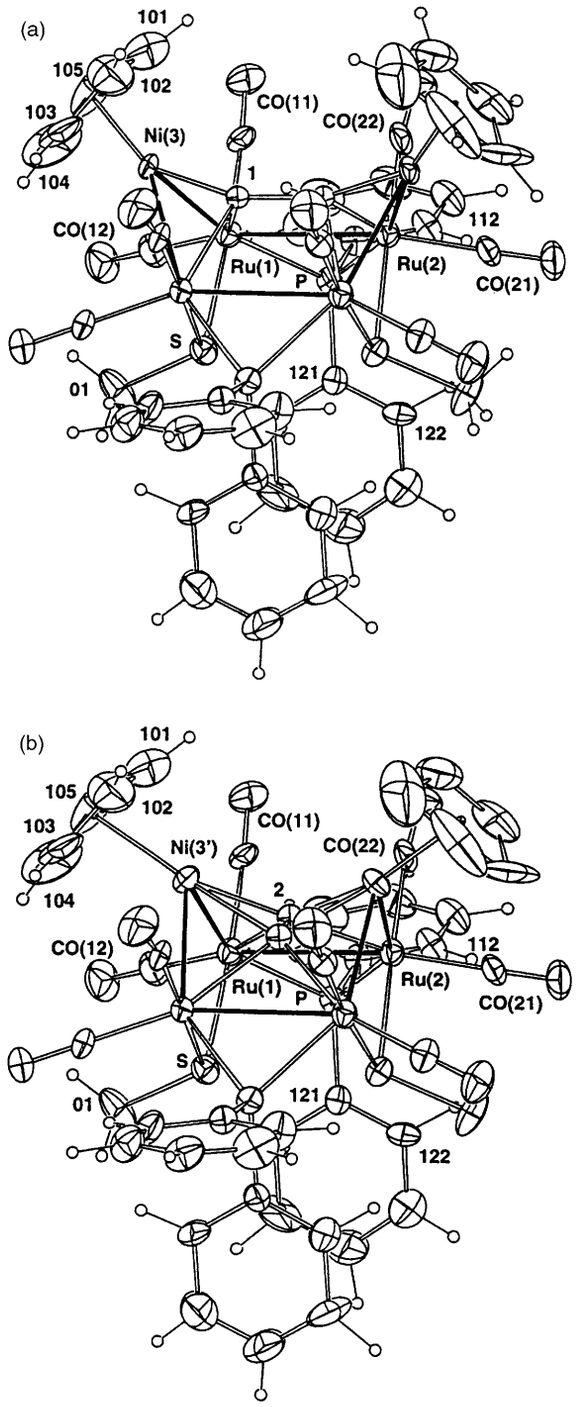

Fig. 2 Projections of $Ni_2Ru_4(\mu_6\text{-}C_2)(\mu\text{-}SMe)_2(\mu\text{-}PPh_2)_2(CO)_8Cp_2$ **13** showing the two molecular components, **13a** and **13b**. 50% Thermal ellipsoids are shown for the non-hydrogen atoms.

interpret the bonding of the C_2 unit to Ru as involving σ-type interactions as found in $Ru_2\{\mu\text{-}\eta^1\text{:}\eta^1\text{-}C_2(CO_2Me)_2\}(CO)_6(Pr^iN{=}CHC_5H_4N)$.[8] The Cp ligand is modelled as ordered, although it would be expected that the thermal envelopes should encompass two components; the Ni(3, 3′)–centroid distances are 1.56(2), 1.98(2) Å, respectively.

Theoretical studies

The electron counts for these two complexes are interesting. Cluster **12** is nearly isostructural with **2**, but lacks the central (hinge) bond found in the latter. Such a species has a cluster valence electron count (c.v.e.) of 96 [5Ru (40) + Ni (10) + 2SMe (6) + $2PPh_2$ (6) + 2Cp (10) + 9CO (18) + C_2 (6)], *i.e.* two more electrons than cluster **2**, as expected for an M_6 cluster with six M–M bonds.[9,10] For **13** the c.v.e. count is also 96 [4Ru (32) + 2Ni (20) + 2SMe (6) + $2PPh_2$ (6) + 2Cp(10) + 8CO (16) + C_2 (6)]. Both clusters may be derived from a trigonal prism (90 c.v.e.) by addition of six electrons. Indeed, the metal cores of **12** and **13** are alternative skeletal arrangements which differ from those reported for the other M_6C_2 clusters mentioned above[10] (see Scheme 2 for a comparison of the metal architecture of these M_6C_2 clusters).

The structural arrangement of the M_6C_2 cluster core in **13** is of particular interest from the viewpoint of the coordination mode of the C_2 entity to a polymetal framework. Indeed, the disorder found in the C_2 location corresponds to the two bonding situations illustrated in structures **13a** and **13b** (see Scheme 1) which may be related to alkyne complexes in which the alkyne is $\mu\text{-}\eta^1\text{:}\eta^1$ [or μ-(‖)] and $\mu\text{-}\eta^2\text{:}\eta^2$ [or μ-(⊥)] with respect to the Ni···Ni vector, and which have been encountered in different C_2-containing clusters.[10] However, in each case, the C_2 fragment is acting as a 6-e donor. Note that structure **13b** is very similar to that of compound **12**.

In order better to understand the bonding of C_2 within its M_6 metallic host in compound **13**, we have calculated and compared the electronic structures of the two arrangements **13a** and **13b**. Density functional (DF) calculations were first carried out. The pertinent metrical parameters obtained from full optimisation performed under the C_2 symmetry constraint are given in Table 2. This was chosen in preference to C_{2v} because of the orientation of the Ph rings on the phosphorus atoms and to allow direct comparison with the crystal structure determinations, which are in C_2 symmetry. Most values compare rather well with the crystallographic data, except for the carbon–carbon distances which are computed at 1.316 and 1.330 Å for **13a** and **13b**, respectively. These computed values seem more valid than those measured experimentally for **13** since they fall better in the range of C–C separations generally measured experimentally for this kind of compound[10] [the C–C distance is 1.328(7) Å in **12** for instance, see above]. These results provide again compelling evidence that DF calculations are reliable for obtaining metrical parameters of organometallic molecules for which experimental structural data are not available or are of poor quality.

A large HOMO–LUMO gap is computed in both cases (1.51 and 1.37 eV for compounds **13a** and **13b**, respectively). Interestingly enough, at the level of accuracy of the method used, both arrangements can be considered as nearly isoenergetic (they are separated by 0.056 eV in favor of structure **13a**). Consequently, it is not surprising that these two arrangements are encountered in the same product.

Extended Hückel (EH) calculations were carried out on models $Ni_2Ru_4(\mu_6\text{-}C_2)(\mu\text{-}SH)_2(\mu\text{-}PH_2)_2(CO)_8Cp_2$ of C_{2v} symmetry (**13-Ha**, **13-Hb**) derived from the DF-optimised structures **13a** and **13b**, in order to analyse qualitatively the bonding between the metallic and carbon moieties in this kind of cluster complex. Indeed, although the C_2 unit binds differently in **13a** and **13b** with respect to the metallic cage, their electronic structures are surprisingly highly comparable.

The EH-MO diagrams of structures **13-Ha** and **13-Hb** are compared in Fig. 3. They were built up from the interaction of the frontier molecular orbitals (FMO) of the $[C_2]^{2-}$ ligand with those of the metallic $[Ni_2Ru_4(\mu\text{-}SH)_2(\mu\text{-}PH_2)_2(CO)_8Cp_2]^{2+}$.[11] The orbital and electronic characteristics of the former are well known.[10] The orbitals that may be involved in interaction with the metallic moiety are illustrated in the middle of Fig. 3. Of the ten valence electrons, eight occupy the σ_u, π_u and σ_g frontier molecular orbitals. Basically, the $[Ni_2Ru_4(\mu\text{-}SH)_2(\mu\text{-}PH_2)_2(CO)_8Cp_2]^{2+}$ metallic fragment of **13-H** consists of two d^8 ML_3 (*i.e.* $[NiCp]^+$)[12] and four d^7 $ML_2L'L''$ [*i.e.* $Ru(CO)_2(\mu\text{-}SH)_{1/2}(\mu\text{-}PH_2)_{1/2}$] entities with L being a terminal two-electron σ donor and L′ and L″ representing two-electron σ-donor ligands equivalent to half a bridging SMe and PPh_2 anion,

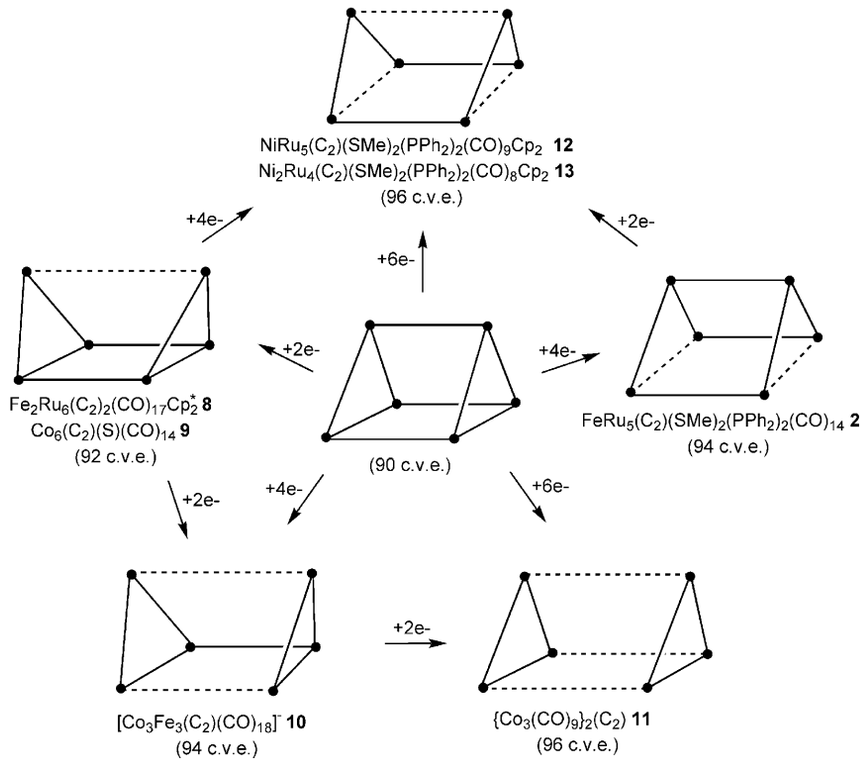

Scheme 2

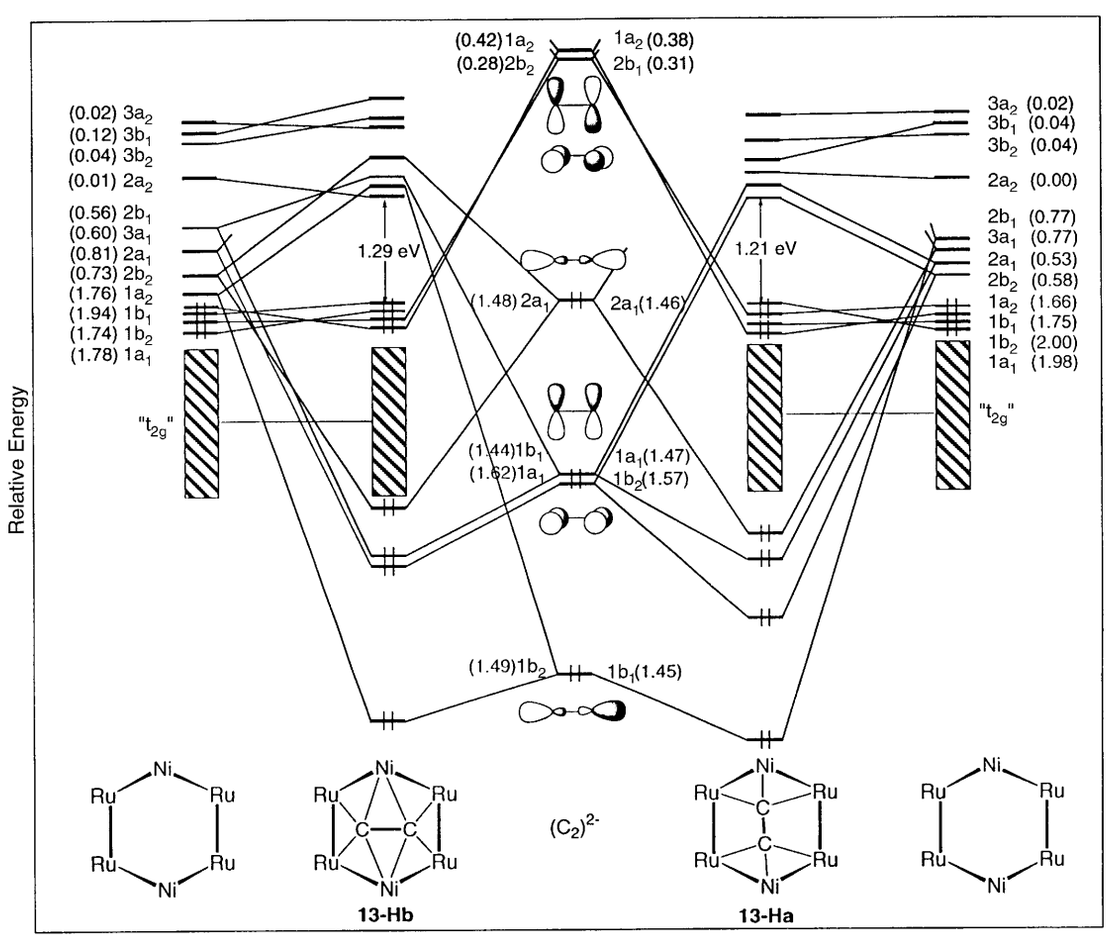

Fig. 3 EH-MO interaction diagram of the model $Ni_2Ru_4(\mu_6\text{-}C_2)(\mu\text{-}SH)_2(\mu\text{-}PH_2)_2(CO)_8Cp_2$ with the C_2 unit either parallel ($\mu_6\text{-}\eta^3:\eta^3\text{-}C_2$; structure **13-Ha**, on the right) or perpendicular ($\mu_6\text{-}\eta^4:\eta^4\text{-}C_2$; structure **13-Hb**, on the left) to the non-bonding Ni···Ni vector. Symmetry labels are given in C_{2v}. The numbers in parentheses indicate the electron occupation of FMOs after interaction.

respectively.[13] Each ML_3 and $ML_2L'L''$ unit possesses three and two FMOs, respectively. A detective analysis reveals that the assemblage of these six units to form the boat-shaped metallic fragment gives rise to 14 hybrid FMOs, above a nest of low-lying, mainly d, orbitals. Among these 14 FMOs, two nickel sp hybrids are very high in energy and can be neglected in a first

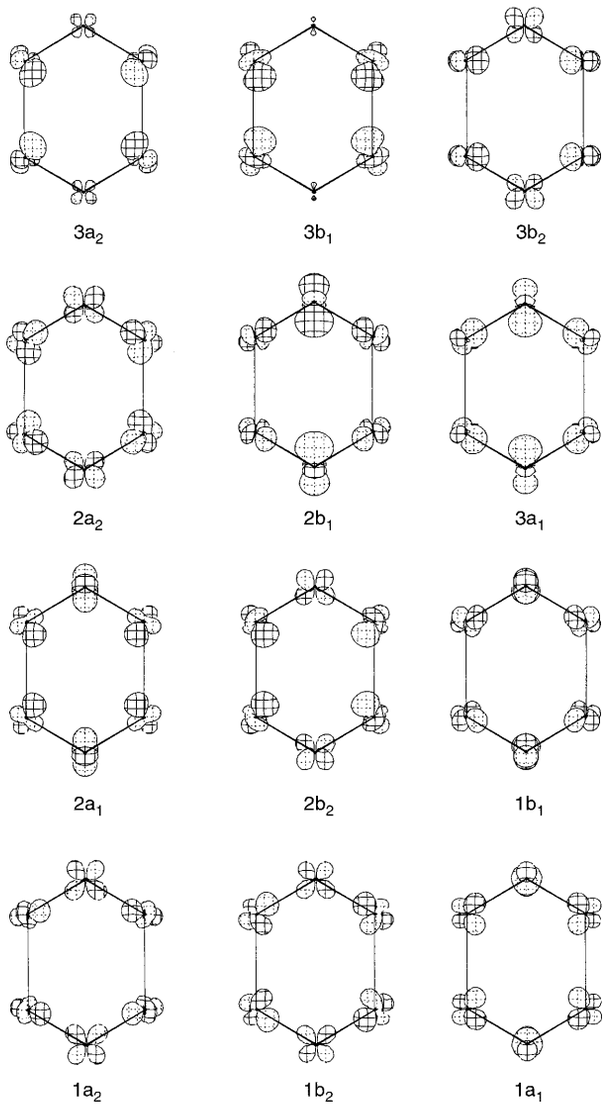

Fig. 4 Frontier molecular orbitals of the metallic $[Ni_2Ru_4(\mu\text{-}SH)_2(\mu\text{-}PH_2)_2(CO)_8Cp_2]^{2+}$ fragment of model **13-Ha** (the FMOs of model **13-Hb** are nearly identical).

approximation. The 12 remaining metallic FMOs, of which four are formally occupied before interaction, are shown in Fig. 4.

Six of the twelve FMOs of the metallic framework interact rather strongly with those of the dicarbon moiety in the (μ_6-η^3:η^3-C_2) structure **13-Ha** (see the right-hand side of Fig. 3). The dominant interactions occur between the formally vacant metallic $2b_1$, $3a_1$, $2a_1$ and $2b_2$ orbitals and the C_2 $1b_1$ (σ_u), $1a_1$ (π_u), $2a_1$ (σ_g) and $1b_2$ (π_u) orbitals, respectively. To a lesser extent, two formally occupied metallic FMOs, namely $1b_1$ and $1a_2$, interact with the acceptor orbitals $2b_1$ and $1a_2$ (π_g*) of the C_2 unit. The six remaining metallic orbitals hardly interact with the C_2 ligand [their electron occupation is close to zero (vacant) or two (occupied) after interaction, see Fig. 3]. These interactions lead to the formation of six occupied M–C bonding MOs corresponding formally to the six M–C bonding contacts in **13a**. Such a cluster can be described as a permetallated ethane, analogous to compounds **8**–**11**.[10]

At first sight the MO diagram of the (μ_6-η^4:η^4-C_2) structure **13-Hb** shown on the left-hand side of Fig. 3 resembles quite strongly that of (μ_6-η^3:η^3-C_2) structure **13-Ha**. Nevertheless, the bonding between the metallic fragment and the C_2 unit in **13-Hb** is more highly delocalised than that in **13-Ha**. This is reflected by the numerous ($\sigma + \pi$)-type interactions between the FMOs of the C_2 and metallic moieties. The main interactions

Table 3 EH computed characteristics for the of (μ_6-η^3:η^3-C_2) **13-Ha** and (μ_6-η^4:η^4-C_2) **13-Hb** model structures

	13-Ha	**13-Hb**
HOMO–LUMO gap/eV		
	1.21	1.29
Atomic net charges		
C	−0.30	−0.34
Ni	0.87	−1.03
Ru	−0.29	−0.33
Overlap populations		
C–C	1.37	1.36
C–Ni	0.63 [2][a]	0.19 [4]
C–Ru	0.24 [4]	0.32 [4]
Ni–Ru	0.12 [4]	0.14 [4]
Ru–Ru	0.09 [2]	0.05 [2]
Ru···Ru	−0.02 [2]	−0.01 [2]

[a] Number of contacts.

involve the metallic FMOs $2b_1$, $2a_1$ and $2b_2$ with the C_2 $1b_1$ and $1a_1$ (π_u), $2a_1$ (σ_g), and $1b_2$ (σ_u) orbitals, respectively (note the change in symmetry labels for the C_2 orbitals in **13-Hb** with respect to **13-Ha**, see the left-hand side of Fig. 3). Other subsequent interactions occur between the vacant metallic $3b_1$ and $3a_1$ FMOs with the C_2 $1b_1$ and $2a_1$ (σ_g) FMOs respectively, as well as between the occupied metallic FMOs $1a_2$, $1b_1$, $1b_2$ and $1a_1$ with the acceptor orbitals $1a_2$ and $2b_2$ (π_g*) and to a lesser extent with occupied C_2 orbitals.

In accord with the DF optimised atomic separations computed in compounds **13a** and **13b**, the C–C EH overlap populations (OPs) are similar in **13-Ha** and **13-Hb** (1.37 *vs.* 1.36) in spite of the different number of C–M bonding contacts. Indeed, the sums of the C–M OPs are similar in **13-Ha** and **13-Hb** (2.24 *vs.* 2.04). Examination of these OPs (Table 3) indicates that each carbon atom of the C_2 unit is firmly σ-ligated to one Ni atom (strong OP: 0.63) and π-bonded to two Ru atoms (medium OP: 0.24) in **13-Ha**, whereas it is π-bonded to two Ni atoms (medium OP: 0.19) and σ/π-bonded to two Ru atoms (rather strong OP: 0.32) in **13-Hb**. OPs corresponding to Ru–Ni and Ru–Ru separations are comparable in both arrangements (see Table 3). As expected, the long Ni···Ni and Ru···Ru contacts are non-bonding.

Despite these very different coordination modes of the C_2 ligand to the metal framework, forward and backward electron donation (see the occupation of the C_2 FMOs after interaction in Fig. 3), atomic net charges and HOMO–LUMO gaps (see Table 3) are comparable for structures **13-Ha** and **13-Hb**. These results further illustrate the flexibility of the C_2 ligand in its bonding to metallic clusters as observed previously for species **2** and **8**–**11**.[10] The computed net electron transfers from the $[C_2]^{2-}$ ligand toward the metal framework (1.41 *vs.* 1.32 electrons) indicate that the bonding of the C_2 ligand with its host is slightly more covalent in **13-Ha** than in arrangement **13-Hb**. Regardless of its coordination mode, the C_2 ligand is slightly negatively charged and therefore would be rather nucleophilic to subsequent charge-controlled reactions.

Discussion

As found in the reactions of compound **1** with $Fe_2(CO)_9$, $Ru_3(CO)_{12}$ and $Co_2(CO)_8$, cluster expansion to give $NiRu_5$ and Ni_2Ru_4 cores occurs when mixtures of **1** with $NiCp_2$ are heated. In the products the C_2 ligand interacts with all six metal atoms. In **12** the Ni atom occupies a hinge position, although the Ni···Ru separation in this case is too long for significant bonding to be present. In **13** a novel disorder is present, in which the C_2 ligand takes up a position either along the

Ni · · · Ni axis or perpendicular to it. The C_2 ligand is too large to be accommodated inside a trigonal prism, so that the open arrangements found here are preferred. We have previously speculated that these reactions occur by attack on **1** at the C_2 ligand with concomitant formation of new M–M bonds (Scheme 1). The first-formed intermediate may collapse by two routes to give either **12** or **13**. Finally, we note that excission of one Ru atom occurs during the formation of **13**. These products are formed in quite low yields, precluding any study of possible intermediates, although a third complex, presently unidentified, is also formed.

Experimental

General reaction conditions

Reactions were carried out under an atmosphere of nitrogen, but no special precautions were taken to exclude oxygen during work-up. Common solvents were dried and distilled under nitrogen before use. Elemental analyses were performed by Canadian Microanalytical Service, Delta, B.C., Canada. Preparative TLC was carried out on glass plates (20 × 20 cm) coated with silica gel (Merck 60 GF_{254}, 0.5 mm thick).

Instrumentation

IR: Perkin-Elmer 1720X FT IR. NMR: Bruker CXP300 or ACP300 (^{1}H at 300.13 MHz, ^{13}C at 75.47 MHz) or Varian Gemini 200 (^{1}H at 199.8 MHz, ^{13}C at 50.29 MHz) spectrometers, with samples dissolved in $CDCl_3$. FAB MS: VG ZAB 2HF (using 3-nitrobenzyl alcohol as matrix, exciting gas Ar, FAB gun voltage 7.5 kV, current 1 mA, accelerating potential 7 kV).

Reagents

Complex **1** was made as previously described.[14] Nickelocene (Strem) was recrystallised (benzene) before use.

Reactions of compound 1 with $NiCp_2$

A solution of compound **1** (100 mg, 0.077 mmol) and $NiCp_2$ (100 mg, 0.53 mmol) in toluene (10 ml) was heated in a Carius tube (120 °C, 1 h). After cooling, solvent was removed and the residue purified by preparative TLC (hexane–acetone 10 : 3) to give three major bands. A dark brown band (R_f 0.45) contained $NiRu_5(\mu_6\text{-}C_2)(\mu\text{-}SMe)_2(\mu\text{-}PPh_2)_2(CO)_9Cp_2$ **12** (8 mg, 7%). Found: C, 37.26; H, 2.29. Calc. for $C_{47}H_{36}NiO_9P_2Ru_5S_2$: C, 39.34; H, 2.53%; IR (cyclohexane): ν(CO) 2031w, 2019vs, 2004vs, 1971m, 1950s, 1947(sh) and 1855w cm^{-1}. FAB MS: *m*/*z* 1436, M^+. The major dark red band (R_f 0.55) contained 45 mg of an as yet unidentified complex. A green band (R_f 0.60) afforded $Ni_2Ru_4(\mu_6\text{-}C_2)(\mu\text{-}SMe)_2(\mu\text{-}PPh_2)_2(CO)_8Cp_2$ **13** (9 mg, 9%; from CH_2Cl_2–MeOH). Found: C, 39.58; H, 2.61. Calc. for $C_{23}H_{18}NiO_4PRu_2S$: C, 40.49; H, 2.66%; IR (cyclohexane): ν(CO) 2027w, 2016vs, 1999s, 1961m and 1949s cm^{-1}. ^{1}H NMR: δ 1.31, 1.65 (2 × s, 3H each, SMe), 5.89, 6.01 (2 × s, 5H each, Cp) and 6.85–7.98 (m, 20H, Ph). FAB MS: *m*/*z* 1365, M^+; 1337–1141, $[M - nCO]^+$ (n = 1–8). A similar reaction carried out at 100 °C for 18 h afforded 15% **13**.

Crystallography

A full sphere of data for compound **12** was measured with a Bruker AXS CCD facility at 153 K to the limit $2\theta_{max} = 50°$. 54877 Reflections merged to 8828 independent (R_{int} 0.037) after 'empirical' absorption correction (proprietary software 'SADABS'), 8219 [$F > 4\sigma(F)$] being used in the refinement. For both structures, anisotropic thermal parameters were refined for the non-hydrogen atoms, (x, y, z, U_{iso})$_H$ being constrained at estimated values. Conventional residuals R, R_w on $|F|$ were 0.051, 0.035 (statistical weights).

A unique data set for compound **13** was measured at *ca.* 295 K to the limit $2\theta_{max} = 50°$ using an Enraf-Nonius CAD4 diffractometer (2θ–θ scan mode, extended counter-arm; monochromatic Mo-Kα radiation, λ 0.7107$_3$ Å); 2561 independent reflections were obtained, 1437 with $I > 3\sigma(I)$ being considered 'observed' and used in the full matrix least squares refinement after gaussian absorption correction. Conventional residuals R, R'_w on $|F|$ were 0.042, 0.034 (statistical weights) for the preferred enantiomer.

Computation used the XTAL 3.4 program system[15] implemented by S. R. Hall; neutral atom complex scattering factors were employed.

Crystal and refinement data. *Compound* **12.** $NiRu_5(\mu_6\text{-}C_2)(\mu\text{-}SMe)_2(\mu\text{-}PPh_2)_2(CO)_9Cp_2 \equiv C_{47}H_{36}NiO_9P_2Ru_5S_2$, monoclinic, space group $P2_1/n$ [C^5_{2h}, no. 14 (variant)], a = 10.909(1), b = 38.870(4), c = 12.001(1) Å, β = 98.577(2)°, V = 5032 Å^3, Z = 4, D_c = 1.89 g cm^{-3}, $F(000)$ = 2800, μ_{Mo} = 20.3 cm^{-1}, specimen 0.55 × 0.30 × 0.10 mm, 'T'$_{min,max}$ = 0.625, 0.867.

Compound **13**. $Ni_2Ru_4(\mu_6\text{-}C_2)(\mu\text{-}SMe)_2(\mu\text{-}PPh_2)_2(CO)_8Cp_2 \equiv C_{46}H_{36}Ni_2O_8P_2Ru_4S_2$, tetragonal, space group $P4_122$ (D^3_4, no. 91), a = 11.416(2), c = 37.328(6) Å, V = 4865 Å^3, Z = 4, D_c = 1.86 g cm^{-3}, $F(000)$ = 2680, μ_{Mo} = 20.0 cm^{-1}, specimen 0.17 × 0.13 × 0.16 mm, $T_{min,max}$ = 0.82, 0.84.

Special features. Ni(3)C(1,2) were modelled as disordered over pairs of sites, occupancy set at 0.5 after trial refinement; the disorder is presumed concerted. Isotropic thermal parameter forms were refined for C(1,2). Meaningful refinement in space group $P4$ was not achieved.

CCDC reference number 186/2300.

See http://www.rsc.org/suppdata/dt/b0/b005210h/ for crystallographic files in .cif format.

Theoretical calculations

DF calculations. Density functional calculations were carried out on compounds **13a** and **13b** using the Amsterdam Density Functional (ADF) program[16] developed by Baerends and coworkers[17] using the local density approximation (LDA) in the Vosko–Wilk–Nusair parametrisation.[18] The atom electronic configurations were described by a triple-ζ Slater-type orbital (STO) basis set for H 1s, C 2s and 2p, O 2s and 2p, P 3s and 3p, S 3s and 3p augmented with a 3d single-ζ polarisation for C, O, P and S atoms and with a 2p single-ζ polarisation for H atoms. A triple-ζ STO basis set was used for Ru 4d and 5s and for Ni 3d and 4s, augmented with a single-ζ 5p polarisation function for Ru or with a single-ζ 4p polarisation function for Ni. A frozen-core approximation was used to treat the core shells up to 1s for C and O, to 2p for P and S, to 4p for Ru and to 3p for Ni.[17] Geometries were optimised using the analytical gradient method implemented by Verluis and Ziegler.[19]

EH calculations. Extended Hückel calculations were carried out within the extended Hückel formalism[20] using the program CACAO.[21] The Slater exponents (ζ) and the valence shell ionisation potentials (H_{ii} in eV) were respectively: 1.3, −13.6 for H 1s; 1.625, −21.4 for C 2s; 1.625, −11.4 for C 2p; 2.275, −32.4 for O 2s; 2.275, −14.8 for O 2p; ; 1.600, −18.6 for P 3s; 1.600, −14.0 for P 3p; ; 1.817, −20.0 for S 3s; 1.817, −13.3 for S 3p; 1.825, −9.11 for Ni 4s; 1.125, −5.15 for Ni 4p; 2.078, −8.60 for Ru 5s; 2.043, −5.10 for Ru 5p. The H_{ii} values for Ni 3d and Ru 4d were at −13.40 and −12.20 respectively. A linear combination of two Slater-type orbitals with exponents ζ_1 = 5.75 and ζ_2 = 2.00 and ζ_1 = 5.378 and ζ_2 = 2.303 with the weighting coefficients c_1 = 0.5683 and c_2 = 0.6292 and c_1 = 0.5340 and c_2 = 0.6365 were used to represent the Ni 3d and Ru 4d atomic orbitals, respectively. EH calculations were carried out on models **13-Ha** and **13-Hb** derived from the averaged DF-optimised geometries of **13a** and **13b**, respectively. The following distances (Å) were used: Ru–Ru 2.967, Ru · · · Ru

3.647, Ru–Ni 2.647, Ru–S 2.468, Ru–P 2.321, Ru–C 2.182 (**13-Ha**) and 2.282 (**13-Hb**), Ru–C(CO) 1.89, Ni–C 1.997 (**13-Ha**) and 1.747 (**13-Hb**), Ni–C(Cp) 2.128, C(Cp)–C(Cp) 1.418, C–O 1.15, C–C(C_2) 1.321, S–H 1.335, P–H 1.42 and C–H 1.09.

Acknowledgements

We thank the Australian Research Council for financial support and Johnson Matthey plc for a generous loan of $RuCl_3 \cdot nH_2O$. Dr Paul Humphrey is thanked for experimental help. These studies were also greatly facilitated by travel grants (ARC IREX programme and the Centre National de la Recherche Scientifique, France). S. K. and J.-F. H. thank the Centre de Ressources Informatiques (CRI) of Rennes and the Institut de Développement et de Ressources en Informatique Scientifique (IDRIS-CNRS) of Orsay for computing facilities.

References

1 C. J. Adams, M. I. Bruce, B. W. Skelton and A. H. White, *J. Organomet. Chem.*, 1998, **551**, 235.
2 C. J. Adams, M. I. Bruce, B. W. Skelton and A. H. White, *Polyhedron*, 1998, **17**, 2795.
3 M. Akita, H. Hirakawa, M. Tanaka and Y. Moro-oka, *J. Organomet. Chem.*, 1995, **485**, C14.
4 M. Akita, S. Sugimoto, M. Tanaka and Y. Moro-oka, *J. Am. Chem. Soc.*, 1992, **114**, 7581.
5 G. Gervasio, R. Rossetti, P. L. Stanghellini and G. Bor, *Inorg. Chem.*, 1984, **23**, 2073.
6 M. P. Jensen, D. A. Phillips, M. Sabat and D. F. Shriver, *Organometallics*, 1992, **11**, 1859.
7 M. D. Brice and B. R. Penfold, *Inorg. Chem.*, 1972, **11**, 1381; U. Geiser and A. M. Kini, *Acta Crystallogr., Sect. C*, 1993, **49**, 1322.
8 F. Muller, G. van Koten, L. H. Polm, K. Vrieze, M. C. Zontberg, D. Heijdenrijk, E. Kragten and C. H. Stam, *Organometallics*, 1989, **8**, 1340.
9 D. M. P. Mingos and A. S. May, in *The Chemistry of Metal Cluster Complexes*, eds. H. D. Kaesz, D. F. Shriver and R. D. Adams, VCH, New York, 1990, ch. 2, p. 11.
10 G. Frapper, J.-F. Halet and M. I. Bruce, *Organometallics*, 1997, **16**, 2590; G. Frapper and J.-F. Halet, *Organometallics*, 1995, **14**, 5044.
11 There are different ways formally to count electrons of the dicarbon moiety. We choose here to consider C_2 as a dianionic rather than a neutral species in order that it agrees with the octet rule. Note that the number of frontier molecular orbitals of C_2 which may participate to the M–C bonding is independent of this electron-counting convention.
12 The charge of the entities constituting the metallic fragment $[Ni_2Ru_4(\mu\text{-}SH)_2(\mu\text{-}PH_2)_2(CO)_8Cp_2]^{2+}$ are chosen arbitrarily.
13 D. G. Evans, *J. Chem. Soc., Chem. Commun.*, 1983, 675; N. Lugan, P.-L. Fabre, D. de Montauzon, G. Lavigne, J.-J. Bonnet, J.-Y. Saillard and J.-F. Halet, *Inorg. Chem.*, 1993, **32**, 1363.
14 C. J. Adams, M. I. Bruce, B. W. Skelton and A. H. White, *J. Chem. Soc., Dalton Trans.*, 1997, 2937.
15 S. R. Hall, G. S. D. King and J. M. Stewart (Editors), *The XTAL 3.4 Users' Manual*, University of Western Australia, Lamb, Perth, 1994.
16 Amsterdam Density Functional (ADF) Program, release 2.0.1, Vrije Universteit, Amsterdam, 1996.
17 E. J. Baerends, D. E. Ellis and P. Ros, *Chem. Phys.*, 1973, **2**, 41; E. J. Baerends and P. Ros, *Int. J. Quantum. Chem.*, 1978, **S12**, 169; P. M. Boerrigter, G. te Velde and E. J. Baerends, *Int. J. Quantum Chem.*, 1988, **33**, 87; G. te Velde and E. J. Baerends, *J. Comput. Phys.*, 1992, **99**, 84.
18 S. D. Vosko, L. Wilk and M. Nusair, *Can. J. Chem.*, 1990, **58**, 1200.
19 L. Verluis and T. Ziegler, *J. Chem. Phys.*, 1988, **322**, 88.
20 R. Hoffmann, *J. Chem. Phys.*, 1963, **39**, 1397; R. Hoffmann and W. N. Lipscomb, *J. Chem. Phys.*, 1962, **36**, 2179.
21 C. Mealli and D. Proserpio, *J. Chem. Educ.*, 1990, **67**, 399.